

## Configuration-Dependent Heat Capacity of Pairwise Hydrophobic Interactions

Seishi Shimizu and Hue Sun Chan\*

Department of Biochemistry and  
Department of Medical Genetics and Microbiology  
Faculty of Medicine, University of Toronto  
Toronto, Ontario, M5S 1A8, Canada

Received September 20, 2000

Revised Manuscript Received January 9, 2001

Hydrophobicity is of central importance to many branches of chemistry, ranging from the low aqueous solubilities of hydrocarbons to properties of polymer solutions, encompassing a broad range of physicochemical and biomolecular phenomena such as the formation of colloid, molecular aggregates, micelles, vesicles, and biological membranes, as well as protein folding and many other self-organization processes.<sup>1–3</sup> Recently, much of the interest in hydrophobic interactions,<sup>2,3</sup> including their modulation by cosolvents,<sup>4</sup> has been motivated by the energetics of proteins and other biomolecules. One of the defining thermodynamic signatures of hydrophobicity is the large and positive heat capacity changes that accompany transfers of nonpolar solutes from pure or nonpolar phases into water.<sup>1</sup> For example, because the unfolding of a protein exposes numerous nonpolar groups to water, it has been widely assumed that the positive heat capacity changes associated with it are closely akin to that of small nonpolar solute hydration.<sup>3,5,6</sup> Characterization of elemental heat capacity effects is thus essential to ascertaining the role of hydrophobic interactions in more complex phenomena. As “bulk” hydrophobic interactions and the interactions among small nonpolar groups in water can be significantly different,<sup>7</sup> to better understand complex hydrophobic phenomena it is necessary to look beyond single-solute hydration and solute transfers between bulk phases. Here we report theoretical calculations of heat capacity effects between pairs of nonpolar solutes, obtained by extensive constant-pressure (NPT) Monte Carlo simulations of TIP4P water<sup>8</sup> under atmospheric pressure. Using data from eight simulation temperatures (278 K, 298 K, 313 K, 328 K, 338 K, 348 K, 368 K, and 388 K), we determine the constant-pressure heat capacity change  $\Delta C_P$  upon bringing a pair of nonpolar solutes from infinity to separations ( $\xi$ ) close to each other. We find that  $\Delta C_P(\xi)$  is significantly nonmonotonic. In particular, at the position of the desolvation free energy barrier ( $\xi \approx 5.7$  Å) of the two-body potential of mean force (PMF),  $\Delta C_P(\xi)$  has a prominent maximum as high as the hydration heat capacity of an entire methane.

We have taken a “brute force” approach to heat capacity.<sup>9</sup> Two-body PMFs [ $\Delta G_P(\xi)$ ] of methanes and hard spheres of the same effective size<sup>10</sup> are computed by test-particle insertions into configurations of 396 waters with periodic boundary conditions. Similar to the methane-methane case,<sup>11</sup> methane–hard-sphere

PMFs are computed by inserting hard spheres to pure water and to water containing one methane. Hard-sphere–hard-sphere PMFs are calculated as follows. For each temperature, after an initial equilibration run of pure water configurations for  $1.3 \times 10^5$  passes, snapshots are collected from at least  $1.3 \times 10^6$  passes ( $1.2 \times 10^7$  passes for 278 K) at an interval of once every 100 passes. Then 40 000–400 000 hard-sphere insertions are attempted per snapshot. If the insertion of the first hard sphere has been successful, 20 000 subsequent insertions of the second hard sphere are attempted.

The PMFs at the eight temperatures are fitted to the relation

$$\text{PMF} = \Delta G(\xi) = \Delta H_0(\xi) + \Delta C_P(\xi)(T - T_0) - T\Delta S_0(\xi) - T\Delta C_P(\xi) \ln(T/T_0) \quad (1)$$

where  $\Delta H_0(\xi)$  and  $\Delta S_0(\xi)$  are enthalpy and entropy changes, respectively, at the reference temperature  $T_0$ . The simplifying assumption here that  $\Delta C_P$  is  $T$ -independent is not unreasonable because experiments suggest that temperature dependences of nonpolar hydration heat capacities are weak.<sup>12</sup> The viability of the present method is supported by two observations: (i) In previous “brute-force” studies, single-methane hydration heat capacity was estimated to be approximately 63 cal/mol/K (264 J/mol/K)<sup>9</sup> and 40 cal/mol/K (168 J/mol/K),<sup>11</sup> in fair agreement with experimental values of 47–53 cal/mol/K (198–223 J/mol/K).<sup>11,12</sup> (ii) The present results for methane–methane, methane–hard-sphere, and hard-sphere–hard-sphere pairs are very similar (see below), lending credence to the robustness of our approach.

Figure 1 shows that: (i) The peak value of  $\Delta C_P(\xi)$  at the desolvation free energy barrier<sup>11</sup> is approximately 46 cal/mol/K (192 J/mol/K);  $-T_0\Delta S_0$  also peaks in the same region. (ii) At the contact minimum,  $-T_0\Delta S_0$  is large and negative. (iii)  $\Delta C_P$  at the contact minimum ( $\xi = 3.8$  Å) and solvent-separated minimum ( $\xi \approx 7.0$  Å) are slightly positive and slightly negative, respectively, but are both close to zero. Observation (iii) underscores the complex relationship between bulk and pair hydrophobic interactions.<sup>7,11,13</sup> While our results agree with experimental data of positive  $\Delta C_P$ 's for nonpolar hydration (see above), Figure 1A contradicts the simplistic expectation based on bulk-phase oil/water transfer data<sup>12</sup> (see below) that bringing two small nonpolar solutes together in water would always result in a significant negative  $\Delta C_P$ .

Our NPT-simulated  $\Delta S_0$  at 3.8 Å is similar in value to its NVT counterparts,<sup>13,14</sup> but is about one-third of that from two studies<sup>15,16</sup> that considered only three temperatures and set PMF to zero at  $\xi = 8$  Å or 8.5 Å. We believe the present results are more reliable because of the effective  $\xi = \infty$  zero-PMF baselines used<sup>11</sup> and the larger number of temperatures simulated. This assessment is buttressed by the observation that the contact-minimum  $\Delta C_P \approx -680$  cal/mol/K reported by ref 16 is unreasonable because it is more than 1 order of magnitude larger than the hydration heat capacity of a single methane.<sup>11</sup>

We compare our results against three common implicit-solvent treatments.<sup>6,17–19</sup> We adopt the working assumption that explicit-

(1) Dill, K. A. *Science* **1990**, *250*, 297–298.  
(2) (a) Kauzmann, W. *Adv. Protein Chem.* **1959**, *14*, 1–63. (b) Tanford, C. *The Hydrophobic Effect: Formation of Micelles and Biological Membranes*; Wiley: New York, 1980.  
(3) (a) Dill, K. A. *Biochemistry* **1990**, *29*, 7133–7155. (b) Blokzijl, W.; Engberts, J. B. F. N. *Angew. Chem., Int. Ed. Engl.* **1993**, *32*, 1545–1579. (c) Hummer, G.; Garde, S.; Garcia, A. E.; Pratt, L. E. *Chem. Phys.* **2000**, *258*, 349–370.  
(4) (a) Wallqvist, A.; Covell, D. G.; Thirumalai, D. *J. Am. Chem. Soc.* **1998**, *120*, 427–428. (b) Vanzi, F.; Madan, B.; Sharp, K. *J. Am. Chem. Soc.* **1998**, *120*, 10748–10753. (c) Shimizu, S.; Shimizu, K. *J. Am. Chem. Soc.* **1999**, *121*, 2387–2394.  
(5) Baldwin, R. L. *Proc. Natl. Acad. Sci. U.S.A.* **1986**, *83*, 8069–8072.  
(6) Makhatadze, G. I.; Privalov, P. L. *Adv. Protein Chem.* **1995**, *47*, 307–425.  
(7) Wood, R. H.; Thompson, P. T. *Proc. Natl. Acad. Sci. U.S.A.* **1990**, *87*, 946–949.  
(8) Jorgensen, W. L. *BOSS*, version 4.1; Yale University: New Haven, CT, 1999.  
(9) Guillot, B.; Guissani, Y. *J. Chem. Phys.* **1993**, *99*, 8075–8094.

(10) We follow the method of Hummer, G.; Garde, S.; Garcia, A. E.; Pohorille, A.; Pratt, L. E. *Proc. Natl. Acad. Sci. U.S.A.* **1996**, *93*, 8951–8955, whereby the closest allowable approach between a “methane-like” hard sphere and a water oxygen is defined as the shortest separation at which the methane–water pair correlation function reaches 1. This distance is 3.3 Å for the TIP4P model used here.  
(11) Shimizu, S.; Chan, H. S. *J. Chem. Phys.* **2000**, *113*, 4683–4700.  
(12) (a) Privalov, P. L.; Gill, S. J. *Adv. Protein Chem.* **1988**, *39*, 191–234. (b) Nagnibhi, H.; Dec, S. F.; Gill, S. J. *J. Phys. Chem.* **1986**, *90*, 4621–4623.  
(13) Lüdemann, S.; Abseher, R.; Schreiber, H.; Steinhauser, O. *J. Am. Chem. Soc.* **1997**, *119*, 4206–4213.  
(14) Smith, D. E.; Haymet, A. D. J. *J. Chem. Phys.* **1993**, *98*, 6445–6454.  
(15) Rick, S. W.; Berne, B. J. *Phys. Chem. B* **1997**, *101*, 10488–10493.  
(16) Rick, S. W. *J. Phys. Chem. B* **2000**, *104*, 6884–6888.  
(17) Lee, B.; Richards, F. M. *J. Mol. Biol.* **1971**, *55*, 379–400.

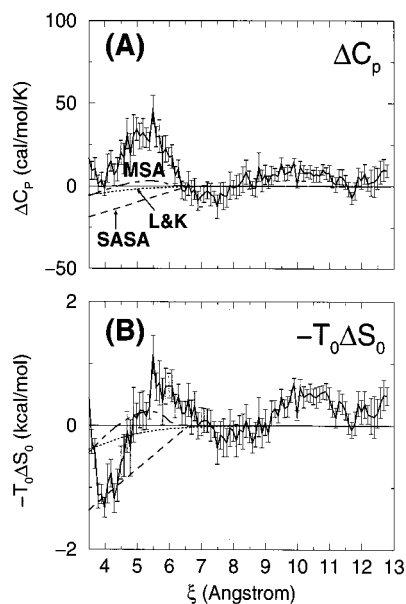


**Figure 1.** (A) Heat capacity  $\Delta C_p$  and (B) entropic free energy  $-T_0\Delta S_0$  ( $T_0 = 298.15$  K) of two-methane association. The bin size used in the calculations is  $0.1 \text{ \AA}$ . Simulation results [thick lines connecting error bars] are compared with predictions by solvent-accessible surface area (SASA),<sup>6,17</sup> molecular surface area (MSA),<sup>18</sup> and a recent Gaussian volume exclusion model of Lazaridis and Karplus (L&K)<sup>19</sup> [line styles defined in (A)]. In these comparisons, the proportionality constants linking surface area and exclusion volume to thermodynamic quantities are set by the simulated hydration heat capacity and entropy of a single methane.<sup>11</sup> Error bars in this communication are deduced as follows. First, for any given  $\xi$ , the full range of PMF error  $2\sigma_i(\xi)$  at each simulation temperature  $T_i$  is defined to be the range between the minimum and maximum PMF values among the last 50 cumulative averages of the calculation taken at intervals of 19 200 passes. Second, least-squares fitting by eq 1 yields a set of coefficients ( $a_i$ 's) such that  $\Delta C_p(\xi) = \sum_i a_i(\xi)[\Delta G_i(\xi)]$ , where  $\Delta G_i(\xi)$  is the simulated (final cumulative average) PMF value at  $\xi$  and temperature  $T_i$ . Hence  $\sigma(\xi) \equiv \sqrt{\sum_i [a_i(\xi)]^2 [\sigma_i(\xi)]^2}$  may be used to estimate the range of error in the fitted  $\Delta C_p(\xi)$ . The error bars in (A) denote  $\Delta C_p(\xi) \pm \sigma(\xi)$ . A similar procedure determines the error bars for  $-T_0\Delta S_0$  in (B).

water results (their limitations notwithstanding) are in large measure better reflections of microscopic features of hydrophobic interactions than models that treat water as a continuum. On the basis of PMF comparisons,<sup>20</sup> we expect robustness of the general trend reported here across commonly employed atomistic water models, although model-dependent variations remain to be investigated. Figure 1 shows that both SASA and L&K predict monotonic decreasing  $\Delta C_p$  with decreasing  $\xi$ . The negative sign of their predicted  $\Delta C_p$  values between  $\xi \approx 4.0 \text{ \AA}$  and  $6.5 \text{ \AA}$  is opposite to that of the simulated results. MSA predicts positive  $\Delta C_p$  in this region, but the predicted magnitudes are roughly an order of magnitude too small. The corresponding implicit-solvent predictions for  $-T_0\Delta S_0$  are also inadequate. The SASA-predicted  $-T_0\Delta S_0$  is quite accurate at the contact minimum, but it fails to predict the desolvation peak. In short, all three implicit-solvent models underestimate the spatial variations of heat capacity and entropy. This is not too surprising because surface area models are known to fail to reproduce well-established hydrophobic PMFs.<sup>11,18</sup>

A dramatic nonmonotonic dependence of  $\Delta C_p$  on pairwise nonpolar solute configuration has potentially far-reaching implications on protein folding.<sup>21</sup> For instance, on the basis of SASA arguments, denatured states of proteins have been asserted to be

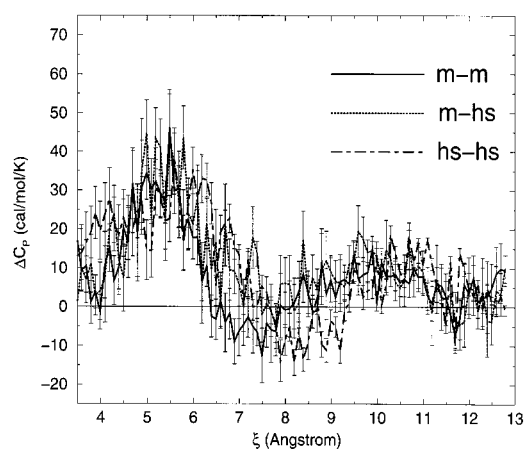


**Figure 2.** Heat capacity  $\Delta C_p(\xi)$  of hydrophobic interactions between a methane pair (**m-m**, same as that in Figure 1), a methane and a hard sphere (**m-hs**) and a pair of hard spheres (**hs-hs**).

random-coil-like, with their amino acid residues fully exposed to water.<sup>6</sup> However, direct experimental measurements indicate that heat-denatured states of proteins are relatively compact,<sup>22</sup> implying that some of their residues may not be fully exposed to water and thus participate in hydrophobic contacts. It is therefore puzzling why the heat capacity of denaturation is well approximated by calculations that assume a fully exposed denatured state.<sup>6</sup> Our predicted configuration-dependent heat capacity effects may help resolve this paradox because Figure 1A indicates that for a pair of *small* nonpolar solutes, inasmuch as heat capacity is concerned, contact formation ( $\xi \approx 3.8 \text{ \AA}$ ) is essentially equivalent to full exposure at large separations ( $\xi > 8.5 \text{ \AA}$ ). Therefore, it may be possible for an ensemble of relatively compact denatured-state conformations with loosely formed hydrophobic contacts to have a heat capacity signature similar to that expected of open random-coil-like conformations.

We have compared methane–methane  $\Delta C_p(\xi)$  with that of methane–hard-sphere and hard-sphere–hard-sphere interactions. Substituting a methane for a hard sphere eliminates the attractive part of solute–water interactions, leaving only hard-core solute volume exclusion and water–water interactions. Figure 2 shows that most salient features of the methane–methane  $\Delta C_p$  persist irrespective of whether there are attractive solute–water interactions. This finding suggests strongly that water–water interactions, a major component of which arises from their hydrogen bonds, are the main driving force responsible for the peculiar behavior of the heat capacity function. Madan and Sharp<sup>23</sup> have applied a random network (RN) model of hydrogen bonding to calculate solvation heat capacities, but their method does not account for two-body  $\Delta C_p(\xi)$ . According to our calculation,<sup>24</sup> the RN-predicted  $\Delta C_p$  at  $\xi = 5.7 \text{ \AA}$  equals approximately  $0.25 \text{ cal/mol/K}$ , which is more than 1 order of magnitude smaller than that in Figure 1A. Currently, we are undertaking further efforts to ascertain a more definitive relation between water structure<sup>3</sup> and the distance-dependent  $\Delta C_p$  reported here.

**Acknowledgment.** We thank Danny Heap for his effort in maintaining our computing system. This work was supported in part by the Connaught Fund. H.S.C. holds a Canada Research Chair.

JA0034390

(21) (a) Chan, H. S. *Proteins* **2000**, *40*, 543–571. (b) Kaya, H.; Chan, H. S. *Proteins* **2000**, *40*, 637–661. (c) Kaya, H.; Chan, H. S. *Phys. Rev. Lett.* **2000**, 4823–4826.

(22) (a) Sosnick, T. R.; Trehwella, J. *Biochemistry* **1992**, *31*, 8329–8335. (b) Hagihara, Y.; Hoshino, M.; Hamada, D.; Kataoka, M.; Goto, Y. *Folding Des.* **1998**, *3*, 195–201. See also: Shortle, D. *Curr. Opin. Struct. Biol.* **1993**, *3*, 66–74.

(23) Madan, B.; Sharp, K. *J. Phys. Chem.* **1996**, *100*, 7713–7721.

(24) This entails applying Madan and Sharp's eqs 7–13 in conjunction with their procedure for scaling RN parameters to the hydrogen-bonding statistics from our simulations.

(18) (a) Jackson, R. M.; Sternberg, M. J. E. *Nature (London)* **1993**, *366*, 638–638. (b) Jackson, R. M.; Sternberg, M. J. E. *Protein Eng.* **1994**, *7*, 371–383.

(19) Lazaridis, T.; Karplus, M. *Proteins* **1999**, *35*, 133–152.

(20) Young, W. S.; Brooks, C. L. *J. Chem. Phys.* **1997**, *106*, 9265–9269.